Long-Haul WDM/SDM Transmission of 40-Gbaud PDM-QPSK over Coupled 4-Core Fibers with Entire 5/4× Oversampling DSP

Manabu Arikawa(1, 2) and Kazunori Hayashi(2)

(1) Advanced Network Research Laboratories, NEC Corporation, 1753 Shimonumabe, Nakahara-ku, Kawasaki, Japan, marikawa@nec.com
(2) Graduate School of Informatics, Kyoto University, Yoshida-honmachi, Sakyo-ku, Kyoto, Japan

Abstract *Long-haul transmission of 40-Gbaud PDM-QPSK signals over 7280-km coupled 4-core fibers is demonstrated with entire 5/4× oversampling DSP including a frequency-domain adaptive 8×8 MIMO filter. The 5/4× oversampling DSP reduces the computational complexity by 34% compared with the conventional 2× oversampling DSP with negligible penalty.*

Introduction

Space-division multiplexed (SDM) transmission is an approach to overcome the capacity limit of long-haul transmission over conventional single-mode fibers (SMFs) [1]. SDM systems with coupled spatial modes provide a high density of channels while coupling between them is allowed. Coupled multi-core fibers (CMCFs) enable low propagation loss and low spatial mode dispersion (SMD) [2], and thus long-haul transmissions have been demonstrated with them [3-6].

SDM systems with coupled modes require an adaptive multi-input multi-output (MIMO) processing on the receiver side to compensate for time-varying spatial coupling and SMD [7], hereinafter referred to as mode demultiplexing. The MIMO filter should have the dimension corresponding to the square of the number of coupled spatial/polarization modes, and the filter length should cover the temporal signal spread due to SMD, which is currently much larger than the polarization mode dispersion of an SMF [2]. Thus, a large adaptive MIMO filter needs to be efficiently implemented for practical SDM systems with coupled channels [5, 8, 9].

One approach to efficiently implement a filter with large temporal spread is a frequency-domain (FD) filter [10, 11], which is widely used for static chromatic dispersion compensation (CDC) in SMF transmission systems [12] and is also investigated for adaptive mode demultiplexing in SDM transmission systems [13-15]. Another approach is to reduce the sampling rate at which a filter operates below conventional 2× oversampling, e.g., fractional 1.5× oversampling, which has been investigated in SMF transmission with a high symbol rate [16-20]. We proposed a FD adaptive filter with fractional oversampling controlled by stochastic gradient descent (SGD) with back propagation. We evaluated it in long-haul transmission over coupled four-core fibers (C4CFs) [21]. In this previous study, we adopted CDC, matched filtering (MF), and sampling timing

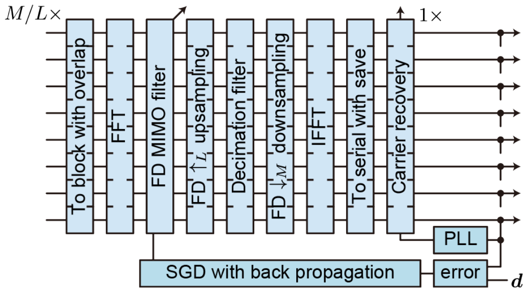

Fig. 1: Fractional *M/L*× oversampling frequency-domain adaptive MIMO filter with overlap-save method.

offset alignment with the timing error [22] at 2× oversampling before fractional *M/L*× oversampling FD adaptive MIMO filter for mode demultiplexing to focus on it. If the entire DSP including CDC/MF and the MIMO filter operates at *M/L*× oversampling, the computational complexity will be further reduced. This possibility has been investigated in SMF transmission [19]. However, the performance penalty when applied to CMCF transmission, in which temporal spread due to SMD is more severe, is not apparent.

In this study, we demonstrated a long-haul WDM/SDM transmission of 40-Gbaud PDM-QPSK signals over C4CFs with entire 5/4× oversampling DSP including CDC/MF and the FD adaptive MIMO filter for mode demultiplexing. Error free transmission after forward error correction (FEC) was achieved up to 7280 km. With an unconstrained FD MIMO filter [8], the entire 5/4× oversampling DSP reduces required complex-valued multiplications by 34% compared with the conventional 2× oversampling DSP with negligible performance penalty.

Entire fractional oversampling DSP for CMCF transmission

Figure 1 shows the fractional *M/L*× oversampling FD adaptive MIMO filter with the overlap-save method [21]. The MIMO filter operates in the FD *M/L*× oversampling, where *M* and *L* are integers. Its outputs are converted to 1× sampling by *L*× upsampling, decimation

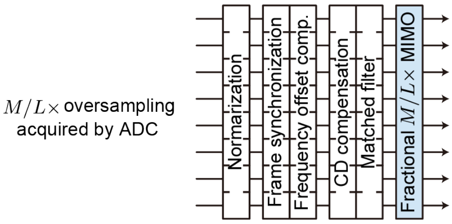

Fig. 2: DSP operating entirely at fractional *M/L*× oversampling for CMCF transmission.

filtering, and 1/*M*× downsampling in the FD. Carrier recovery (CR) is performed on the signals converted to the time-domain (TD) 1× sampling. The coefficients of the FD MIMO filter are controlled by SGD and gradient calculation with back propagation through the sampling rate conversion to minimize the least-mean square (LMS) loss consisting of an error between the output signals in the TD 1× sampling and a training (or decision-directed) symbols ***d***. A phase-locked loop (PLL) is used to control the phase rotation of CR.

We consider here the case in which the sampling rate of an analog-to-digital converter (ADC) is *M/L*× oversampling and the entire DSP including CDC/MF before the FD MIMO filter operates at *M/L*× oversampling, as shown in Fig. 2. After the *M/L*× oversampling signals acquired by the ADC after coherent reception are normalized, frame synchronization to use the data-aided algorithm for the FD adaptive MIMO filter is performed together with frequency offset compensation [21]. Then, CDC and MF operating at *M/L*× oversampling are performed. CDC/MF are assumed to be executed by one static FD filter with overlap-save. The signals after CDC/MF are the inputs of the *M/L*× oversampling FD MIMO filter. In this DSP architecture, sampling timing alignment [22], which was used in our previous study, is simply omitted. It can be recovered by an appropriate adaptive filter [23].

The computational complexity of the entire fractional *M/L*× oversampling DSP is estimated in terms of required complex-valued multiplications. We have estimated the computational complexity of the fractional *M/L*× oversampling FD adaptive MIMO filter [21]. That of the static FD filters for CDC/MF operating at *M/L*× oversampling can be estimated similarly. However, the required filter lengths, i.e., overlap sizes of FD filters, for CDC/MF and mode demultiplexing are usually different in CMCF transmission. We consider a long-haul C4CF transmission, and we set the filter lengths for CDC/MF and mode demultiplexing to 2048 and 256 symbols, respectively. We set *M/L* = 5/4 as used later.

Figure 3 shows the estimation of required complex-valued multiplications per symbol. We

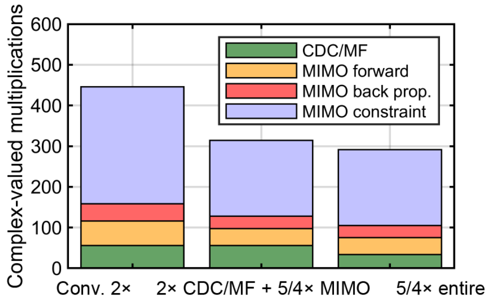

Fig. 3: Required complex-valued multiplications per symbol.

compared three DSP architectures; (i) both CDC/MF and the FD adaptive MIMO filter operate at 2× oversampling that corresponds to a conventional DSP (Conv. 2×); (ii) CDC/MF operates at 2× oversampling and the 5/4× oversampling FD adaptive MIMO filter is used (2× CDC/MF + 5/4× MIMO); and (iii) the entire DSP including CD/MF and the FD adaptive MIMO filter operates at 5/4× oversampling (5/4× entire). With a constraint to avoid the penalty due to assuming the periodicity of a signal block in the FD adaptive MIMO filter [11], 5/4× entire architecture reduces multiplications by 35% from Conv. 2× and by 7% from 2× CDC/MF + 5/4× MIMO. It is suggested that this constraint can be omitted with a small performance penalty for CMCF transmission [14]. In this unconstrained case, 5/4× entire reduces multiplications by 34% from Conv. 2× and by 18% from 2× CDC/MF + 5/4× MIMO.

Transmission experiment

A long-haul WDM/SDM transmission of 40-Gbaud PDM-QPSK signals over C4CFs was demonstrated with a 50 GS/s ADC and the entire 5/4× oversampling DSP. The experimental setup is shown in Fig. 4, which is similar to our previous one [21] except for using 40-Gbaud signals.

The 40-Gbaud PDM-QPSK signal at 193.3 THz for evaluation was generated with a 92-GS/s digital-to-analog converter (DAC). The transmitted data consisted of FEC frames of the low-density parity-check for DVB-S2 with a frame length of 64,800 and a code rate of 0.8 with random bits in the payload. Root-raised cosine filtering with a roll-off factor of 0.1 was used. The remaining 15 channels from 192.90 to 193.65 THz in a 50-GHz grid were generated similarly with a 64-GS/s DAC. After channel power equalization by a wavelength selective switch (WSS) and low-speed polarization scrambling (PS), SDM signals were emulated by dividing WDM signals into four and decorrelating them.

The transmission line was a recirculating loop consisting of two spans of 52-km C4CF with parallel EDFAs, and WSSs for gain/loss equalization for WDM channels. The averaged propagation loss, effective core area, and SMD

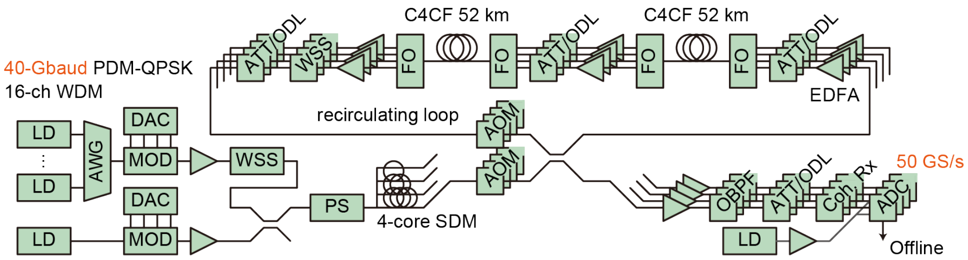

Fig. 4: Experimental setup for WDM/SDM transmission of 40-Gbaud PDM-QPSK signals over C4CFs with entire 5/4× oversampling DSP. AOM: acousto-optic modulator, FO: fanout, ATT: optical attenuator, ODL optical delay line.

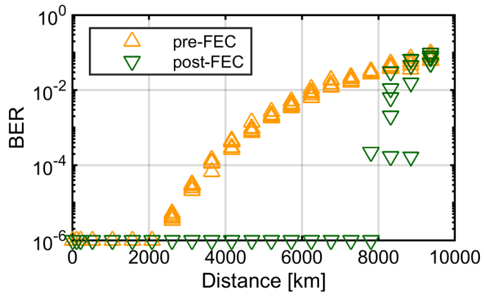

Fig. 5: Pre- and post-FEC BERs after transmission.

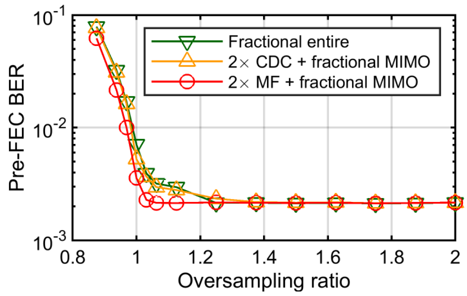

Fig. 6: Dependence of pre-FEC BER on oversampling ratio after 5200-km transmission.

of C4CFs were 0.165 dB/km, 112 μm^2, and 6.9 ps/√km. The span input optical power was set to +1 dBm/ch/core. The averaged optical signal-to-noise ratio was 36.5 dB/0.1 nm after two-span transmission.

After transmission, the signals under evaluation were demultiplexed by optical bandpass filters (OBPFs). The outputs of coherent receivers were sampled by a 16-channel 50-GS/s ADC. Received waveforms were acquired five times for each condition. Offline DSP with the entire 5/4× oversampling configuration shown in Fig. 2 was performed. The coefficients of the FD MIMO filter are controlled with the data-aided LMS loss for pre-convergence first and then switched to the decision-directed LMS. The FD adaptive MIMO filter was unconstrained.

Figure 5 shows the pre- and post-FEC BER after transmission with the entire 5/4× oversampling DSP. BERs for five waveform acquisitions averaged over eight spatial and polarization modes were plotted at each distance. Error-free transmission after FEC was achieved up to 7280 km. Five waveform acquisitions resulted in similar pre-FEC BERs, which indicated that the FD adaptive MIMO filter well compensated for the sampling timing offsets.

Finally, the impact of the oversampling ratio *M/L* on the performance of the entire fractional oversampling DSP was evaluated in detail. We compared three configurations; (a) the signals were resampled to *M/L*× oversampling after frame synchronization. CDC/MF and the FD adaptive MIMO filter operated all at *M/L*× oversampling (Fractional entire); (b) the signals were resampled to 2× oversampling after frame synchronization. CDC operated at 2× oversampling. Then the signals were resampled to *M/L*× oversampling. MF and the FD adaptive MIMO filter operated all at *M/L*× oversampling (2× CDC + fractional MIMO); and (c) CDC and MF was interchanged in case (b) (2× MF + fractional MIMO). In all cases, the filter lengths were fixed, i.e., 2048 symbols for CDC/MF and 256 symbols for mode demultiplexing.

Figure 6 shows the pre-FEC BER after 5200-km transmission with the three configurations while changing the oversampling ratio. Results of five acquisitions were averaged. A small penalty down to 1.1× oversampling was observed with 2× MF + fractional MIMO. Fractional entire and 2× CDC + fractional MIMO showed negligible penalty down to 1.25× oversampling.

Conclusions

We demonstrated a long-haul WDM/SDM transmission of 40-Gbaud PDM-QPSK signals over 7280-km C4CFs with the entire 5/4× oversampling DSP including CDC/MF and the FD adaptive MIMO filter for mode demultiplexing. The entire 5/4× oversampling DSP reduces required complex-valued multiplications by 34% compared with the conventional 2× oversampling DSP with negligible performance penalty.

Acknowledgements

This work was partially supported by the National Institute of Information and Communications Technology, Japan (01001), and the Japan Society for the promotion of science KAKENHI (JP22H00514). We thank Masaki Sato for his support.

References

[1] D. J. Richardson, J. M. Fini, and L. E. Nelson, "Space-division multiplexing in optical fibres," *Nature Photonics*, **7**, 354 (2013), DOI: 10.1038/nphoton.2013.94.

[2] T. Hayashi, Y. Tamura, T. Hasegawa, and T. Taru, “Record-low spatial mode dispersion and ultra-low loss coupled multi-core fiber for ultra-long-haul transmission”, *J. Light. Technol.*, **35**(3), 450 (2017), DOI: 10.1109/JLT.2016.2614000.

[3] R. Ryf, J. C. Alvarado-Zacarias, S. Wittek, N. K. Fontaine, R.-J. Essiambre, H. Chen, R. Amezcua-Correa, H. Sakuma, T. Hayashi, and T. Hasegawa, “Coupled-core transmission over 7-core fiber”, in *Optical Fiber Communication Conference (OFC)*, 2019, Th4B.3. DOI: 10.1364/OFC.2019.Th4B.3.

[4] D. Soma, S. Beppu, Y. Wakayama, S. Sumita, H. Takahashi, N. Yoshikane, I. Morita, T. Tsuritani, and M. Suzuki, “50.47-Tbit/s standard cladding coupled 4-core fiber transmission over 9,150 km”, *J. Light. Technol.,* **39**(22), 7099 (2021). DOI: 10.1109/JLT.2021.3109890.

[5] S. Beppu, M. Kikuta, K. Igarashi, H. Mukai, M. Shigihara, Y. Saito, D. Soma, H. Takahashi, N. Yoshikane, T. Tsuritani, I. Morita, and M. Suzuki, “Long-haul coupled 4-core fiber transmission over 7,200 km with real-time MIMO DSP”, *J. Light. Technol.,* **40**(6), 1640 (2022). DOI: 10.1109/JLT.2022.3147477.

[6] M. Arikawa, M. Wu, K. Yasuhara, D. Masuda, K. Hayashi, T. Inoue, and Y. Inada, “Long-haul WDM/SDM transmission over coupled 4-core fibers installed in submarine cable”, *J. Light. Technol.,* **41**(6), 1649 (2023). DOI: 10.1109/JLT.2022.3229123.

[7] M. Mazur, N. K. Fontaine, S. Corteselli, H. Chen, L. Dallachiesa, T. Hayashi, H. Sakuma, T. Hasegawa, R. Ryf, and D. T. Neilson, “Comparison of transfer matrix stability between a 110 km 7-core coupled-core muple-core fiber and single-mode fiber”, in *Optical Fiber Communication Conference (OFC)*, 2022, M1E.2. DOI: 10.1364/OFC.2022.M1E.2.

[8] S. Randel, S. Corteselli, D. Badini, D. Pilori, S. Caelles, S. Chandrasekhar, J. Gripp, H. Chen, N. K. Fontaine, R. Ryf, and P. J. Winzer, “First real-time coherent MIMO-DSP for six coupled mode transmission”, in *IEEE Photonics Conference*, 2015, 1. DOI: 10.1109/IPCon.2015.7323761.

[9] M. Mazur, L. Dallachiesa, N. K. Fontaine, R. Ryf, E. Börjeson H. Chen, H. Sakuma, T. Ohtsuka, T. Hayashi, T. Hasegawa, H. Tazawa, D. T. Neilson, and P. Larsson-Edefors, “Real-time transmission over 2×55 km all 7-core coupled-core multi-core fiber link”, in *Optical Fiber Communication Conference (OFC)*, 2022, Th4A.1. DOI: 10.1364/OFC.2022.Th4A.1.

[10] J. J. Shynk, “Frequency-domain and multirate adaptive filtering”, *IEEE Signal Processing Magazine,* **9**(1), 14 (1992). DOI: 10.1109/79.109205.

[11] S. Haykin, *Adaptive filter theory fourth ed.* (Prentice Hall, 2002).

[12] R. Kudo, T. Kobayashi, K. Ishihara, Y. Takatori, A. Sano, E. Yamada, H. Masuda, Y. Miyamoto, and M. Mizoguchi, “Two-stage overlap frequency domain equalization for long-haul optical systems”, in *Optical Fiber Communication Conference (OFC)*, 2009, OMT3. DOI: 10.1364/OFC.2009.OMT3.

[13] N. Bai and G. Li, “Adaptive frequency-domain equalization for mode-division multiplexed transmission”, *IEEE Photon. Technol. Lett.,* **24**(21), 1918 (2012). DOI: 10.1109/PHOSST.2012.6280725.

[14] S. Randel, P. J. Winzer, M. Montoliu, and R. Ryf, “Complexity analysis of adaptive frequency-domain equalizer for MIMO-SDM transmission”, in *European Conference on Optical Communication (ECOC)*, 2013, Th.2.C.4. DOI: 10.1049/cp.2013.1540.

[15] K. Shibahara, T. Kobayashi, and Y. Miyamoto, “Out-of-band exclusive frequency-domain MIMO equalization with the reduced-overlap-and-save method for scalable mode multiplexed signal transmission”, *Opt. Express,* **31**(2), 2302 (2023). DOI: 10.1364/OE.475258.

[16] F. Pittalà and J. A. Nossek, “Efficient frequency-domain fractionally-spaced equalizer for flexible digital coherent optical receivers”, in *European Conference on Optical Communication (ECOC)*, 2015, P.3.14. DOI: 10.1109/ECOC.2015.7341751.

[17] S. F. A. Shah, L. Wang, C. Li, and Z. Zhang, “Low-complexity design of noninteger fractionally spaced adaptive equalizers for coherent optical receivers”, *IEEE Signal Processing Lett.,* **23**(9), 1289 (2016). DOI: 10.1109/LSP.2016.2584780.

[18] C. Li, Z. Zhang, J. Chen, T. Ding, Z. Xiao, F. Shah, J. Mitra, H. Xiang, and X. Cui, “Advanced DSP for single-carrier 400-Gb/s PDM-16QAM”, in *Optical Fiber Communication Conference (OFC)*, 2016, W4A.4. DOI: 10.1364/OFC.2016.W4A.4.

[19] M. Paskov, D. S. Millar, and K. Parsons, “A fully-blind fractionally-oversampled frequency domain adaptive equalizer”, in *Optical Fiber Communication Conference (OFC)*, 2016, Th2A.33. DOI: 10.1364/OFC.2016.Th2A.33.

[20] F. Hamaoka, S. Okamoto, M. Nakamura, A. Matsushita, T. Kobayashi, H. Yamazaki, M. Nagatani, Y. Kisaka, A. Hirano, and Y. Miyamoto, “Experimental demonstration of simplified adaptive equalizer for fractionally sampled 120-GBaud signal”, in *European Conference on Optical Communication (ECOC)*, 2017, P1.SC3.34. DOI: 10.1109/ECOC.2017.8345917.

[21] M. Arikawa and K. Hayashi, “Frequency-domain adaptive MIMO filter with fractional oversampling using stochastic gradient descent for long-haul transmission over coupled 4-core fibers”, *Opt. Express,* **31**(8), 13104 (2023). DOI: 10.1364/OE.486032.

[22] F. M. Gardner, “A BPSK/QPSK timing-error detector for sampled receivers”, *IEEE Trans. On Commun.,* COM-34(5), 423 (1986). DOI: 10.1109/TCOM.1986.1096561.

[23] K. Kikuchi, “Clock recovering characteristics of adaptive finite-impulse-response filters in digital coherent optical receivers”, *Opt. Express,* **19**(6), 5611 (2011). DOI: 10.1364/OE.19.005611.